Earthquake Engineering, Tenth World Conference © 1992 Balkema, Rotterdam. ISBN 90 5410 060 5

RC columns in cyclic biaxial bending and axial load

S.N. Bousias
CEC, Institute of Safety Technology, JRC Ispra, Italy & University of Patras, Greece

G. Verzeletti & G. Magonette
CEC, Institute of Safety Technology, JRC Ispra, Italy

M.N. Fardis
University of Patras, Greece

ABSTRACT: The experimental behaviour of slender flexure-dominated reinforced concrete columns in eight biaxial load paths under constant axial load is described. Results show strong coupling between the two directions of bending, which increases energy dissipation, as well as between them and the axial direction.

1 INTRODUCTION

The force-deformation behaviour and failure of reinforced concrete columns under cyclic biaxial bending and axial load is important for the three-dimensional response of r.c. structures to bidirectional ground motions. Recent years have seen the development of various analytical/numerical biaxial models for columns. The scarcity of test data for various biaxial load paths is a limiting factor for the further development and calibration of such models. This paper presents the results of a test program which aims at supplementing the available experimental information (Kobayashi et al, 1980, Li et al, 1988, Low & Moehle, 1987, Saatcioglou & Ozcebe, 1989, Takizawa & Aoyama 1976). The program refers to a single specimen geometry and reinforcement, selected so that shear deformations and bond-slip effects are insignificant, and the behavior is governed by bending and axial load. During each test the axial load is essentially constant and approximately the same in all the tests. The program focuses on the effect of the biaxial load path.

2 TEST SPECIMENS AND RESULTS - DISCUSSION

The cantilever-type specimens have a length of 1.5m and a 0.25mx0.25m square cross-section and are reinforced with eight 16mm bars, and two 8mm square ties at a 70mm spacing (Fig. 1). Bars are deformed, with yield and tensile strengths equal to 440MPa and 660MPa respectively, and ultimate elongation 11%. Concrete cylinder strength at the time of testing ranges between 25MPa and 33MPa. Transverse and axial loads are applied at the tip of the cantilever. Longitudinal bars are anchored well in the heavily reinforced 0.5m thick base of the specimen.

TEST No.1 (f_c=31MPa, $\nu = N/Af_c$=-0.15): Tip displacement is constant in transverse direction X, and is cycled in transverse direction Y, at a linearly increasing amplitude up to the level of the X displacement (Fig. 2a). Hysteresis loops in direction Y exhibit a slight degradation with a step-increase of the X displacement (Fig. 2d). Due to coupling between the two directions, the force required in direction X to maintain constant the X displacement drops continuously with the cycling in direction Y, and needs to be reversed to reduce the X displacement to zero before its increase to the next level of constant displacement (Fig. 2c). Mean vertical displacements exhibit a slight and gradual axial shortening when only the axial load is applied, and a significant axial extension which accompanies the transverse displacements and seems proportional to a value between the sum of the absolute values of transverse displacements and their vector resultant (Fig. 2b). It is noteworthy that the axial extension due to 2 half-cycles of the same amplitude, is much larger in the first than in the second.

TEST No.2 (f_c=28MPa, ν=-0.03, ν=-0.15): Imposed transverse displacement paths are circular, consisting of 4 cycles at each level of resultant displacement at about 20, 50, 80 and 110mm. The normalized axial load ν is equal to 0.03 during the cycles at the first two displacement levels and to 0.15 during the last two. Measured force paths are also quasi-circular, but exhibit a large degradation of strength and stiffness with cycling at the higher transverse displacement levels, leading eventually to complete failure (Fig. 3b). The phase-lag between transverse force and displacement resultants, the sine of which equals the damping ratio, remains nearly constant during cycling at each level of transverse displacement, increasing from about 8^0 at 20mm displacement, to 25^0 at 50mm, 35^0 at 80mm and 45^0 at 110mm (Fig. 3c). Axial extensions are nearly proportional to resultant transverse displacements

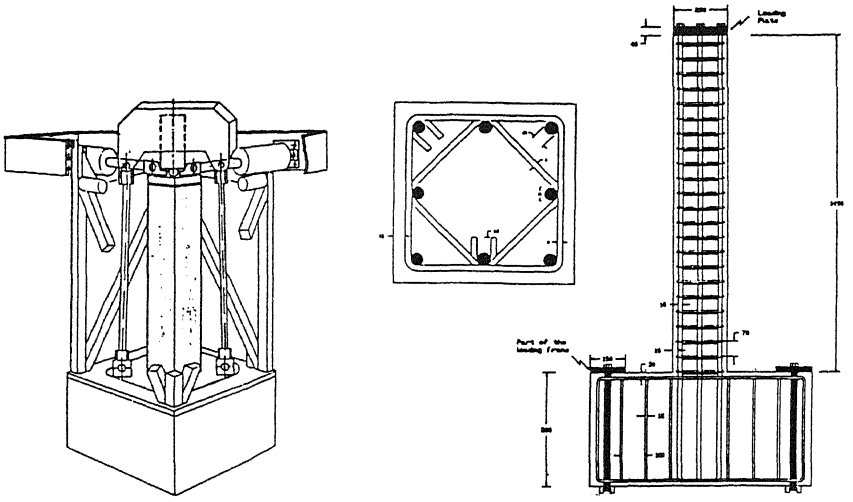

Figure 1. Experimental setup and specimen geometry and reinforcement

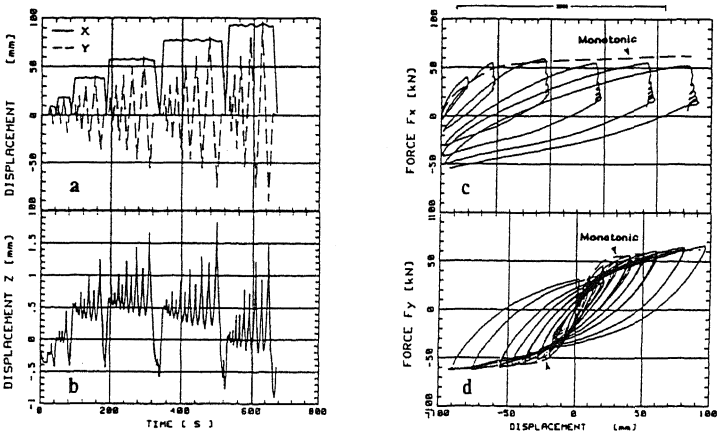

Figure 2. Test 1: (a) Imposed transv. displacements; (b) Vert. displacement; (c), (d) Hysteresis loops.

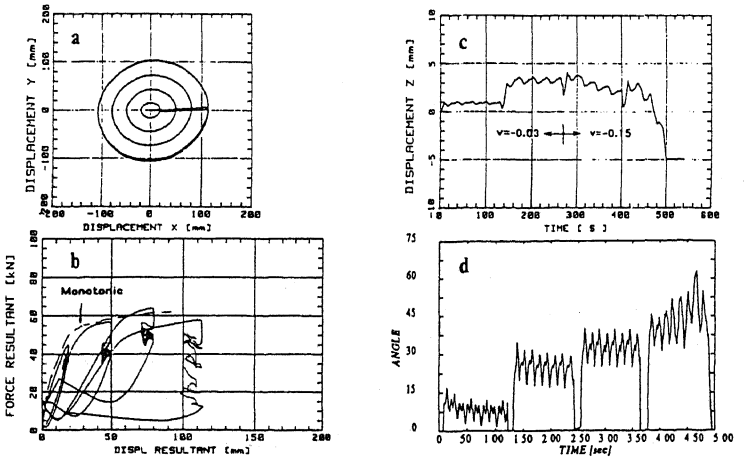

Figure 3. Test 2: (a) Imposed displ. paths; (b) Measured resultant force vs. imposed resultant displacement; (c) Phase-lag between measured force and imposed displacements; (d) Vert. displacement.

during the first two transverse displacement levels. However, as we approach failure during the last two transverse displacement levels, the gradually accelcrating shortening due to the higher axial load dominates over the extension (Fig. 3d).

TEST No.3 (f_c=30MPa, ν=-0.17) and 4 (f_c=28 MPa, ν=-0.15): As shown in Fig. 4a, in these tests the force in transverse direction Y is kept constant while 3 cycles of linearly increasing displacement amplitude are applied in direction X, for each constant level of force Y. Test No.5 differs from No.4 in that each level of force Y is applied first in the positive and then in the negative sense, with repetition of the displacement X cycling. In both tests the force in direction Y causes some degradation of stiffness in direction X (Fig. 4c). The displacement cycles in X cause a gradual but significant increase in the Y displacement under constant Y force (Fig. 4d). In Test No.5, the reversal of this latter force reduces the ratcheting displacements in its direction. The effect of transverse displacements on the axial ones (Fig. 4b) is the same as that observed in Test No.1.

TEST No.5 (f_c=26MPa, ν=-0.12) and 6 (f_c=33 MPa, ν=-0.10): As shown in Fig. 5a, in these tests the imposed transverse displacement path consists of nested cycles of a) uniaxial displacement in direction X up to point 1 or 1', etc., b) uniaxial displacement in direction Y equal to 100% (Test No.5) or 50% (Test No.6) of that in direction X, while keeping the X displacement constant (point 2 or 2'), c) proportional unloading to zero displacement in both directions (point 0), d) proportional loading in both directions, at 1:1 displacement ratio in Test No.5 or 2:1 in Test No.6, up to the maximum previous values of displacement in the opposite sense (point 3 or 3'), e) reduction to zero of the Y displacement under constant X displacement (point 4 or 4') and f) uniaxial unloading to zero in direction X, etc. So the two symmetric halves of the path are traced in the opposite sense. As shown in Fig. 5b, the biaxial force paths are not similar to the corresponding displacement paths. Branches of the force path are rotated with respect to the corresponding ones of the displacement path. The rotation is such that the direction of the displacement path is intermediate between the one of the corresponding branch of the force path and that of the immediately previous branch of the load or of the displacement path. The nested force paths converge to the same points at 1, 1', etc. and 3, 3', etc. where the (degraded) biaxial failure envelope seems to be reached. Symmetric points of the type 2 and 3 on the displacement path correspond to completely nonsymmetric ones on the force path: At the end points 3 of diagonal loading, the forces in the two directions are proportional to the corresponding displacements, whereas at point 2, which is reached by incrementing displacements seperately in each direction, the force in the subsequent direction of loading (Y) is disproportionately larger, as the force in the prior direction of loading (X) is reduced during deformation in direction Y. Hysteresis loops in the two directions X and Y are significantly different, with the exception of the parts corresponding to the proportional unloading/reloading branches of the type 2-0-3. The force drop along branches of the type 1-2 and 2-3 widens the loops and significantly increases the amount of dissipated energy. This increase in energy dissipation is related to the rotation of the branches of the force path with respect to the ones of the displacement path, and is due to the coupling of the response between the two transverse directions. Transverse displacements induce an axial extension roughly proportional to their resultant and a reversal of the shortening due to the axial load into gradually increasing stretching (Fig. 5e). So, as shown also in the early part of Test No.2 and by the axial displacement results of the two tests to be described next, if the axial load is low cycling of the transverse displacements produces gradually a net (i.e. at zero transvesre displacement) axial extension, which may turn into shortening only when failure is imminent.

TEST No.7 (f_c=25.5MPa, ν=-0.12) and 8 (f_c=28MPa, ν=-0.11): Imposed transvesre displacement paths have the form of nested expanding (in Test No.7) or shrinking (in Test No.8) squares. The rotation of the branches of the resulting force paths with respect to the corresponding ones of the displacement paths follows the pattern discussed above for tests No.5 and 6, is due to the coupling between the directions (reduction in the force in one direction under constant displacement, due to the change, positive or negative, of the displacement in the transverse direction) and results in increased energy dissipation (cf. the widening of the unloading branches in Fig. 6c). In Test No.7 the "squares" of the force paths almost coincide, although the force point is well inside the biaxial failure envelope of the column. On the contrary, in Test No.8 the shrinking of the nested displacement paths produces a nearly proportional shrinking of the force paths. In both tests a full revolution on the displacement path, back to the starting point 1 or 1' of uniaxial displacement, leads to a different end point on the force path, and actually to one at which force Y is not zero (as at the starting point) but equal to force X. Finally, the variation of mean axial deformations follow the same pattern as in previous tests (Fig. 6d).

3 CONCLUSIONS

The coupling ot the response in the two orthogonal directions of bending is significant and results in increased energy dissipation. For the levels of axial load applied herein, biaxial or uniaxial transverse displacements induce an axial extension on the column, which is roughly proportional to their vector resultant. At the same time the cycling of transverse displacements causes a ratcheting shortening of the column under axial load alone (ie. at zero lateral displacement) for normalized axial loads ν beyond about -0.15 or a ratcheting extension, which turns

into rapid shortening when failure is approached, for ν less than -0.12.

REFERENCES

Kobayashi, Y., Takiguchi, K., Kokusho, S. & Kimura, M. 1980. Response of R/C columns to horizontal bi-directional deflection history. *Proc. 7th WCEE* : 6, 403-410., Instabul.

Li,K-N, Aoyama, H. & Otani, S. 1988. Reinforced concrete columns under varying axial load and bi-directional lateral load reversals. *Proc. 9th WCEE*: 8, 537-542., Tokyo.

Low, S. & Moehle, J.P. 1987. Experimental study of reinforced concrete columns subjected to multiaxial cyclic loading. UCB/EERC-87/14, Univ. of Cal., Berkeley.

Saatcioglou, M. & Ozcebe, G. 1989. Response of reinforced concrete columns to simulate seismic loading. *ACI Struct. J.*: 80-S1, 3-12.

Takizawa, H. & Aoyama, H. 1976. Biaxial effects in modeling earthquake Response of R/C structures. *Int. J. Earthq. Eng. Struct. Dyn.*: 523-552.

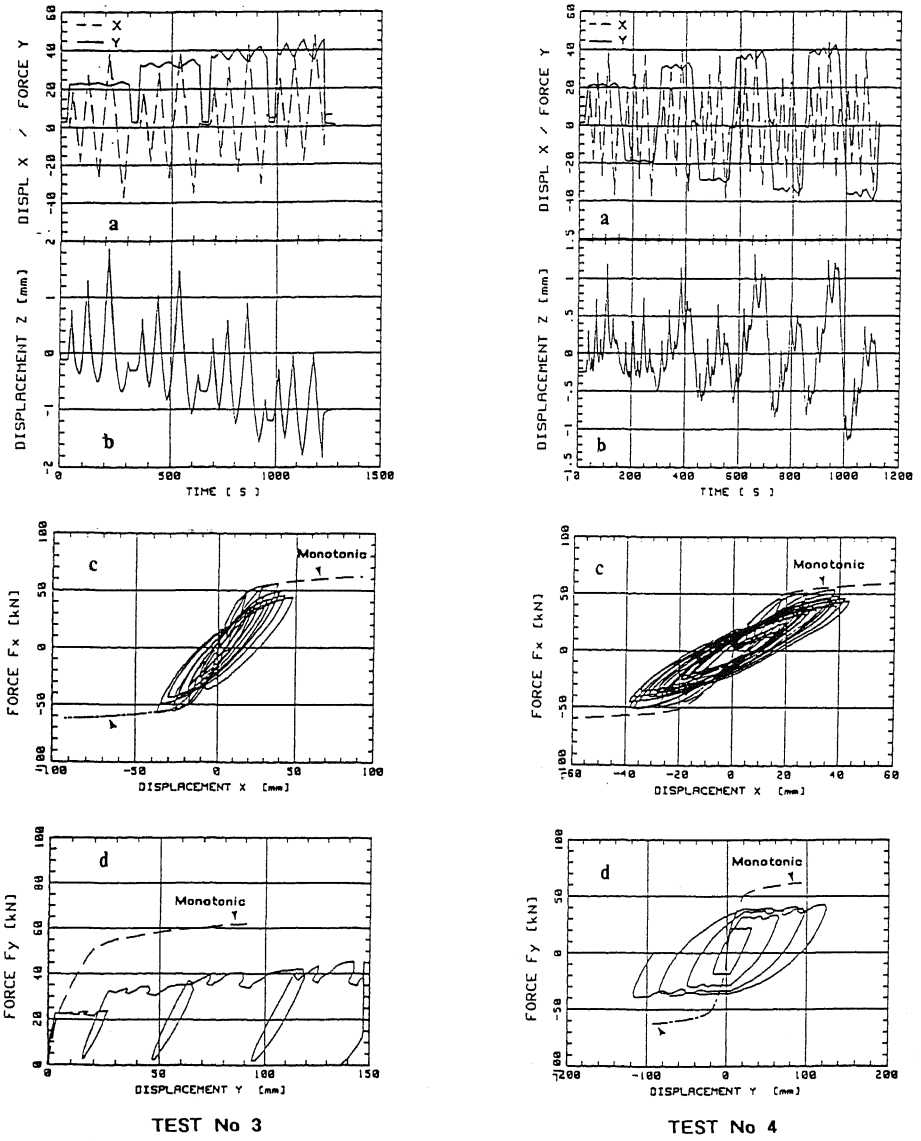

Figure 4. Tests 3 and 4: (a) Imposed displ. paths; (b) Vert. displacement; (c), (d) Hysteresis loops.

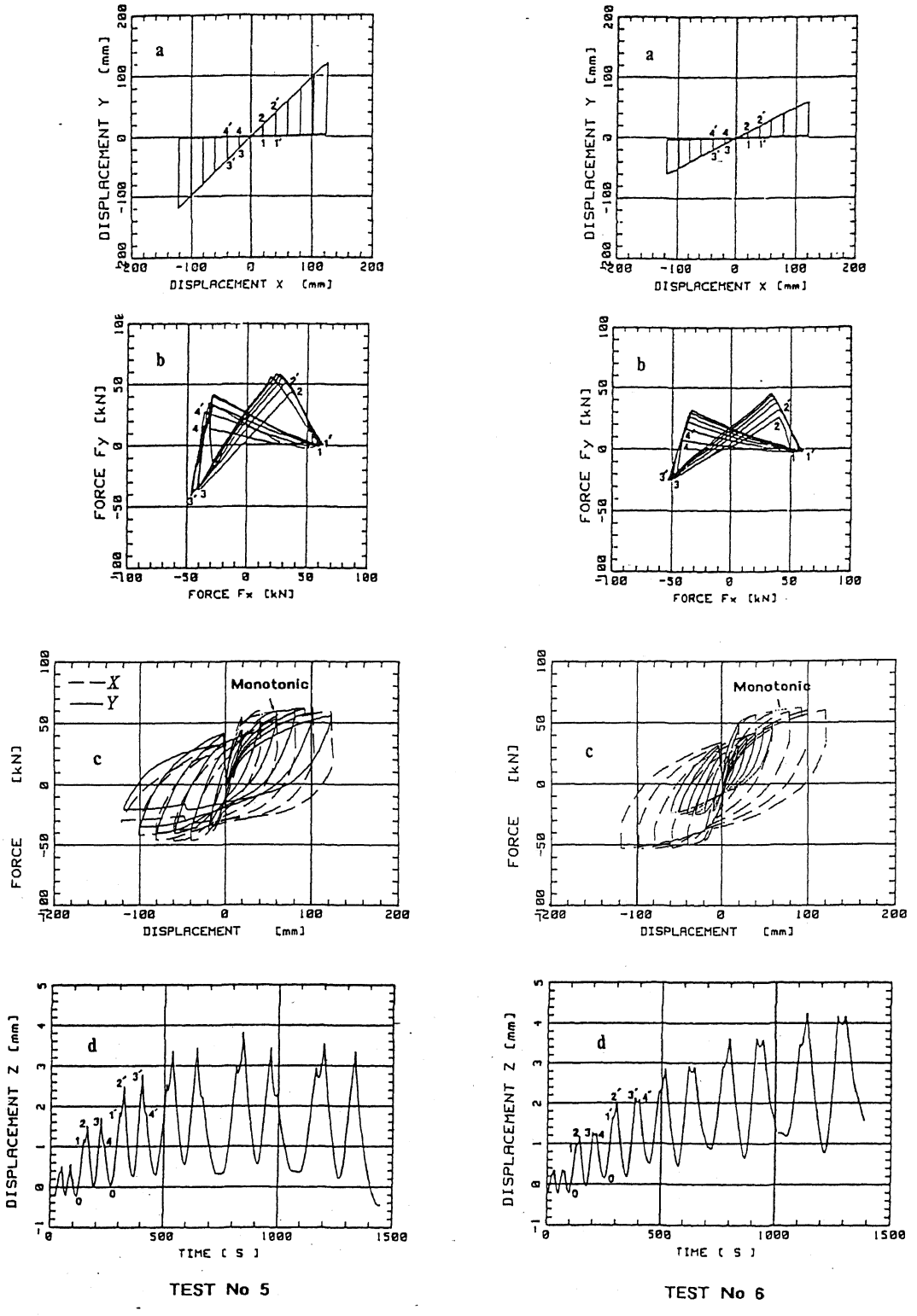

Figure 5. Tests 5 and 6: (a) Imposed displ. paths; (b) Measured force paths; (c), (d) Hysteresis loops; (e) Vert. displacement.

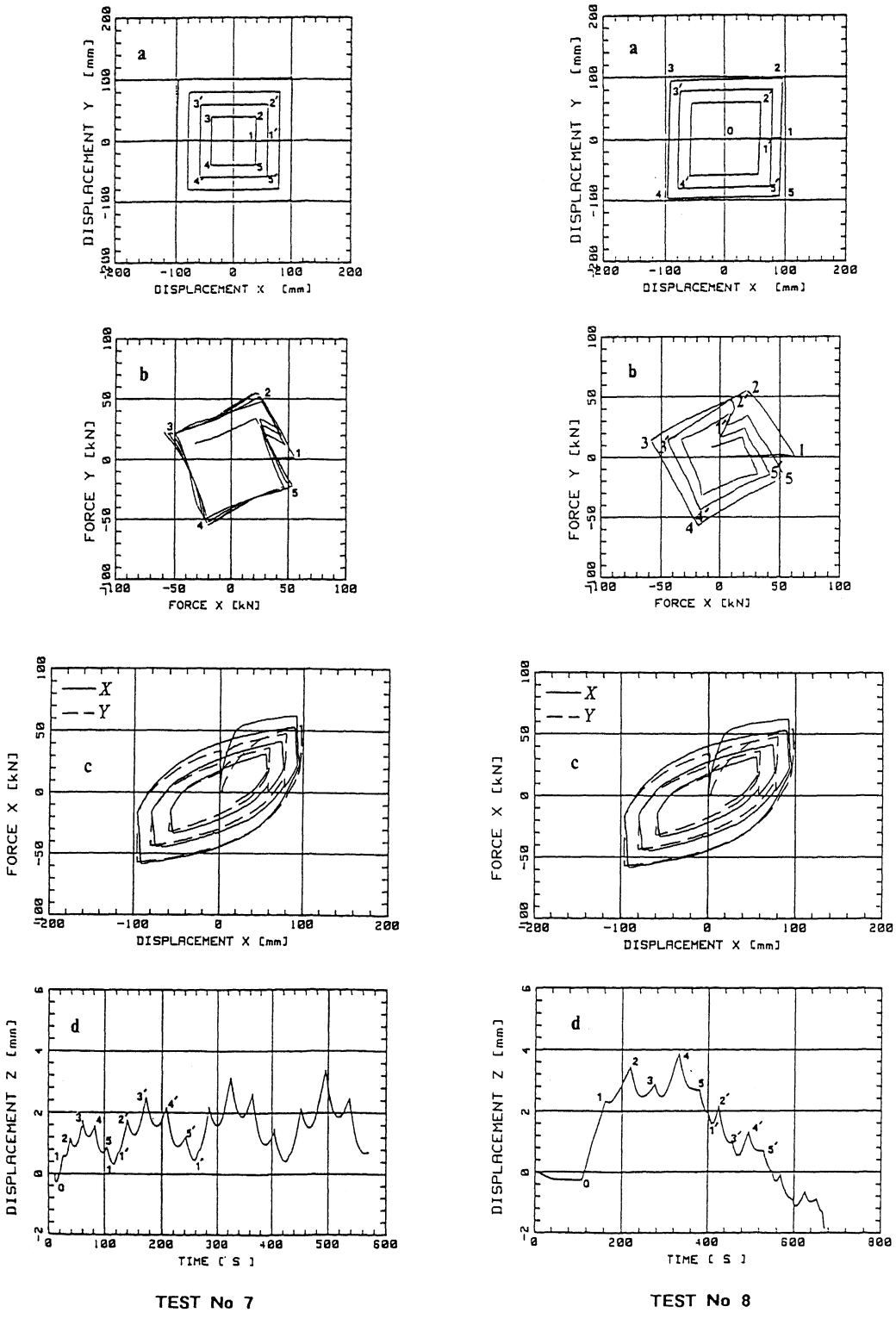

Figure 6. Tests 7 and 8: (a) Imposed displ. paths; (b) Measured force paths; (c), (d) Hysteresis loops; (e) Vert. displacement.